

Deakin Research Online

Deakin University's institutional research repository

This is the published version (version of record) of:

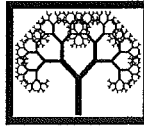
Gao, Weimin, Kong, Lingxue and Hodgson, Peter 2004, Computational simulation of heat transfer from alternate heating sources, *in Proceedings of the 4th International Conference on Engineering Computational Technology*, Civil-Comp, Kippen, Scotland, pp. 1-9.

Available from Deakin Research Online:

<http://hdl.handle.net/10536/DRO/DU:30005569>

Every reasonable effort has been made to ensure that permission has been obtained for items included in DRO. If you believe that your rights have been infringed by this repository, please contact drosupp@deakin.edu.au

Copyright : 2004, CI-Premier



Computational Simulation of Heat Transfer from Alternant Heating Sources

W.M. Gao[†], L.X. Kong[‡] and P.D. Hodgson[†]

[†]School of Engineering and Technology
Deakin University, Geelong, Australia

[‡]Centre for Advanced Manufacturing and Research
University of South Australia, Mawson Lakes, Australia

Abstract

The alternant heat transfer induced by particle packet and gas bubbles on an object surface in a gas fluidised bed is computationally studied. The particle packet and bubble are modelled by a DPPM (double particle-layer and Porous Medium) model and a hemispherical model, respectively. Different meshing schemes are applied and different mesh sizes are used in meshing particle packet and heated object and a very large geometrical size difference between them was considered. Two parallel solver processes were proposed to perform the simulation of heat transfer for different purposes and implemented with the Fluent CFD package.

Keywords: periodic heat transfer, computational model, computational procedure, implementation, user defined function.

1 Introduction

The heat transfer from alternant heating sources to an object is a thermo-physical phenomenon that can be found in many industrial processes for various purposes, including chemical, pharmaceutical, petroleum, agricultural, biochemical, food, electronic, energy, and metallurgical technologies. The heating of an immersed object in a fluidised bed can be considered as the heat transfer from two alternant heating sources—particle packet and bubbles.

The fluidised bed has been widely used in many industrial applications by transforming fine solids into a fluid-like state through contact with a gas phase [1, 2]. On the basis of the two-phase theory of fluidisation [3, 4], a dense bubbling fluidised bed has some low solid density regions called bubbles and a higher density region called the particle packet or emulsion. Therefore, the heat transfer between the fluidised bed and the surface of an immersed object is contributed by the emulsion and bubble phases, which alternately contact with the immersed surface, as shown in Figure 1.

The heat transfer between the emulsion phase and the immersed object strongly depends on the population and behaviours of the particles in contact with the object. Generally, the solid particles that have been widely used have a mean size of 40~500 μm and a density of 1000~4000 kg/m^3 . The void in the emulsion can be presented by the voidage, which is in the range of 0.42~0.60, depending on the gas fluidising velocity and the physical properties of the particles. The heat transfer from the emulsion phase includes particle conduction, gas convection and radiations in the case of a high temperature operation [4-6].

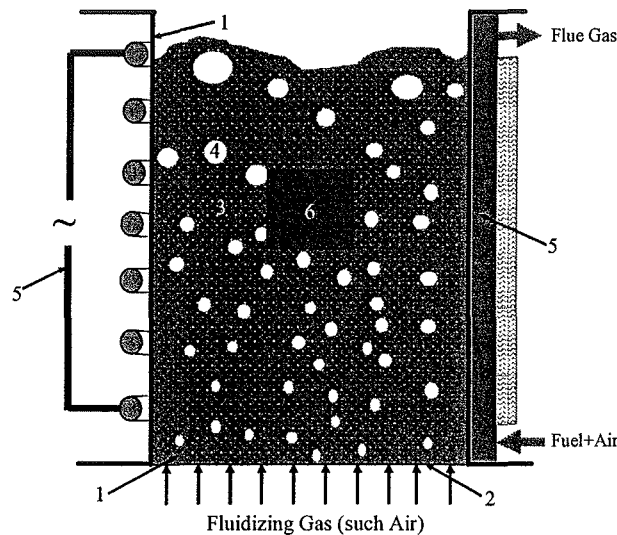


Figure 1. Fluidised bed and immersed object

- 1—fluidised bed; 2—gas distributor; 3—emulsion phase; 4—bubble phase;
 5—heating equipment (right: flue combustion heating; left: electric heating);
 6—immersed object

Bubbles in a fluidised bed can be quite irregular in shape and may vary greatly in size, d_b . The judgement of bubble shape and a suitable magnitude for d_b depends upon having observed bubbles with the particular type of bed being considered [7]. For Geldart B particles [8], the bubble size is about several centimetres. The rising velocity and the fraction of bubbles in bed are mainly influenced by fluidising gas velocity and determine the emulsion residence time, $\tau_{r,p}$, and bubble residence time, $\tau_{r,b}$, on the immersed surface and as a result, affect the heat transfer rate.

In the present paper, the heat transfers from emulsion and bubble phases is modelled by a double particle layers and porous medium model and a hemispherical model, respectively. The simulation of the heat transfer is performed by alternately renewing the boundary conditions relating to the particle packets and gas bubbles, and implemented into Fluent CFD package via parallel solvers.

2 Modelling

The heat transfer to an immersed object is performed by the particle packets and gas bubbles. They sweep the object surface alternately (Figure 2). The heat transfer from emulsion and bubbles is simulated by using different models.

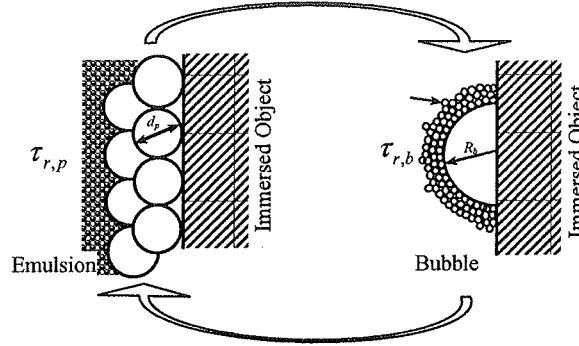


Figure 2. Heat transfer models

2.1 Heat transfer from emulsion

A model called DPPM [9], which contains two particle layers and a porous medium (Figure 2), was proposed to model the emulsion phase and used to calculate the radiative parameters of emulsion, such as view factor, and the contributions of conduction, convection and radiation. The conductive heat transfer occurs in the gas-film regions which are around the contact points of the particles to the immersed surface. On other areas, the heat transfer between the emulsion phase and the immersed surface is dominated by convection from the moving gas. The area of the conduction surface of the immersed object strongly depends on the diameter of the particles [10]. For a specific arrangement of particles near the immersed surface, the following area fraction (f_a) of conduction surface to the total heat-transfer surface is a function of particle diameter and can be given by

$$f_a = \frac{0.0544}{(1 + r_e)^2 d_p^{0.6}} \quad (1)$$

where, r_e is the expansion ratio of particle arrangement (%).

Therefore, the mechanisms contributing to heat transfer between the emulsion and the immersed surface include conduction through the gas-film with the area fraction of f_a , gaseous convection on other surface of the immersed object, and radiation in the case of high temperature operation. Total heat flux during the emulsion contact is

$$q_w = f_a q_{cond,e} + (1 - f_a) q_{conv,e} + q_{r,e} \quad (2)$$

2.2 Heat transfer from bubbles

A bubble in contact with the immersed surface is enclosed by only two surfaces, the concave surface of the emulsion phase and the surface of the immersed object. The bubbles can be considered as being transparent, because the radiation mean-free-path length in the gas phase was much greater than the usual bubble diameters [11]. Therefore, the heat transfer between the bubble and the immersed surface is due to the gaseous convection and radiation that takes place between the internal concave surface of the bubbles and the immersed surface. The total heat flux during bubble contact is

$$q_w = q_{conv,b} + q_{r,b} \quad (3)$$

In order to simulate the heat transfer between bubbles and the immersed surface, it is necessary to have the shape of the bubbles in contact with the surface of the immersed object. However, because of the complexity introduced by various factors like bubble size distribution, bubble shape that is usually distorted by the presence of the immersed surface, and the large number of positions in which an individual bubble can interact with the immersed surface, there are various possible bubble geometries. In the present work, the hemispherical bubble (Figure 2) proposed by Yoshida et al. [11] was adopted.

3 Implementation of the simulation

3.1 Mesh of models

The differences in the sizes of emulsion phase, hemispherical bubble and the immersed object are very obvious and cannot be disregarded in building and meshing a corresponding 3-D geometry (Table 1). The emulsion phase is small ($0.6 \times 0.276 \times 0.216 \text{ mm}^3$) for particles with an average diameter of 0.1 mm; the hemispherical bubble is bigger than the emulsion phase and is 15mm in radii; the immersed object is much larger than emulsion phase and hemispherical bubble. It is not practical to mesh them with approximately the same mesh size and combine the three geometries, which tends to have a low computational accuracy in solving the models. Therefore, it is preferable to simulate the heat transfer in three models, respectively.

Objects	Emulsion phase	Bubble phase	Immersed object
Geometry	Gas-solid mixture	Gas bubble	Bolt
Characteristic Size	0.05~0.5mm	~100mm	30~84mm
Model	DPPM	Semi-sphere model	Solid Model
Model Size	(height×width×depth) $0.6 \times 0.276 \times 0.216 \text{ mm}^3$	15mm in radii	Same as geometry
Mesh Types	TGrid	--	Hexahedral
Mesh Size	0.005~0.01mm	--	2mm

Table 1. Characteristics parameters of the models and mesh

In order to simplify the problem, the heat transfer in the hemispherical bubble model was theoretically calculated in simulation. Therefore, only the DPPM model and the immersed object were meshed and the heat transfers were simulated with finite difference method.

For DPPM model, the TGrid type of meshing scheme was applied (Figure 3a). Most of the mesh elements are tetrahedral, some are hexahedral pyramidal and wedge. There is a very large geometrical size difference in the gas domain. The spaces near the contact points of particle-to-particle and particle-to-immersed surface are very small, while that in the porous medium region is large (Figure 3b). Therefore, different mesh sizes were used for different regions. A larger mesh with an elemental size of $d_p/10$ was used for the region of the second layer particles and the porous medium while a smaller one, $d_p/20$, was acceptable for meshing the immersed surface and the surfaces of first-layer particles. As a result, the elemental size increases with the distance between the immersed surface and the first-layer particle surfaces (Figure 4). This is important to calculate the heat transfer in the gas region near the contact points of the particles to the immersed surface, and to reduce the number of elements. A too coarse mesh will lead to the generation of low-quality elements, which can be examined by Gambit [12], and an over-prediction of the heat transfer. The use of a too fine mesh in the whole domain will result in the generation of a huge number of elements, which requires a considerable computational effort. After meshing, the number of cells, faces and nodes used in this work is 507,871, 1,045,621 and 99,924, respectively.

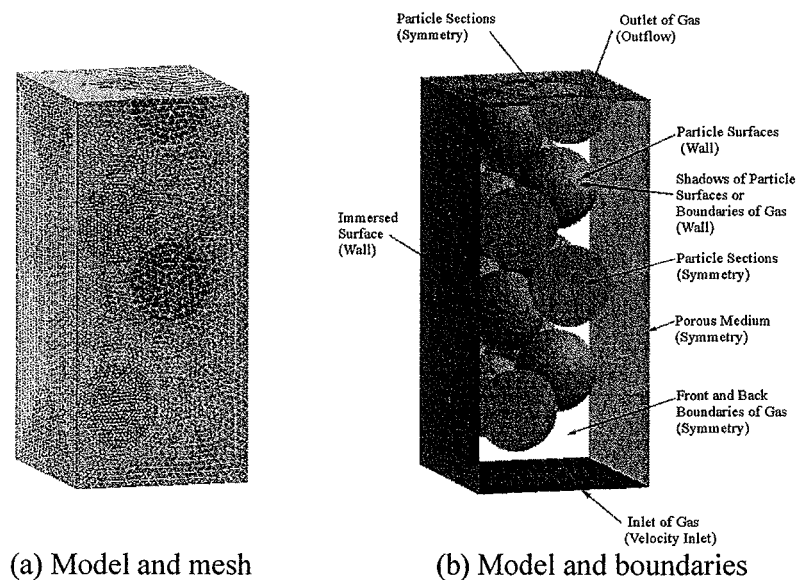


Figure 3. Mesh and boundary conditions of the DPPM model

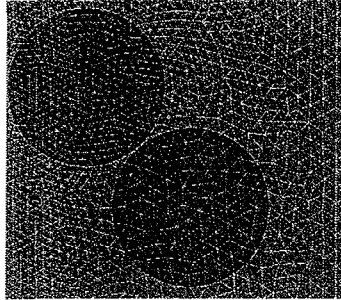


Figure 4. The meshing size of the DPPM model

An immersed bolt with a geometry shown in Figure 5 in fluidised bed was used to simulate the heat transfer. The material is SAE1025. The hexahedral element was used in meshing the bolt. The meshes of bolt surface in depth of 2 mm were refined by a 0.05 mm first row and a growth factor of 1.05. In the centre of the bolt, the spacing size of 2 mm was used in meshing (Figure 5).

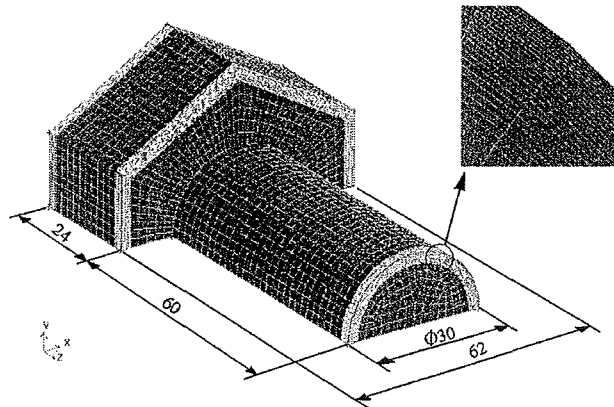


Figure 5. Mesh of the workpiece

3.2 Solver

A parallel solver was performed to compute the solution by using two processes that executed on two networked computers. Figure 6 illustrates two architectures of the parallel solver.

The first parallel process (Figure 6. a) was designed to focus on computing the instantaneous heat-transfer rate on the surface of immersed object. The heat diffusion within immersed object and heat transfer from bubble phase are performed on one computer, while the heat transfer from emulsion is simulated on another computer. The parallel simulation processes are identified by integer IDs. The temperature of the immersed surface is shared by different models and the data interaction between the models is performed through a library built in the computer 1. As “communicators”, the process IDs and heating time are also stored in the

library and used to control the performance of the simulation processes. The operations, such as printing, displaying messages, and writing to a file, can be performed on both computers.

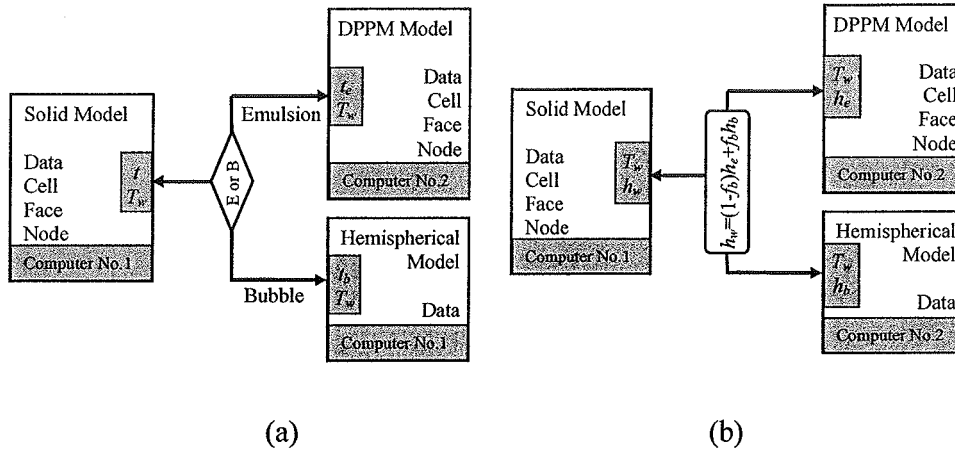


Figure 6. Parallel simulation Architecture

The instantaneous heat-transfer rate on the surface of an immersed object in a fluidised bed varies during the emulsion or bubble contact. To model transient phenomenon properly, it is necessary to set the calculation time step, Δt , at least one order of magnitude smaller than the smallest time constant in the system being modelled for time-dependent problems [13]. Under fluidization, the contact time of the emulsion phase with the immersed surface is very short, normally in the range of 0.1-0.5 s [14]. Hence, the time step, Δt , used in the first parallel process, is in the range of 0.01-0.05 s.

However, 0.01-0.05 s is not necessary in simulating the heat transfer within the immersed object. If the heating process of the immersed object is considered as the purpose of simulation, the variation of the instantaneous heat-transfer rate during the emulsion residence time can be neglected. It is more practical to consider an average heat-transfer coefficient in a heat-transfer period, $\tau_{r,e} + \tau_{r,b}$, (in this period the emulsion and the bubble sweep the heat exchange surface, alternately), in order to reduce the computational time.

The second parallel process (Figure 6. b) was used to implement the simulations. In this process, different time steps are adopted. In simulating the heat transfer between the emulsion and the immersed surface, the time step is the same as the first parallel process, while a time step of 1.0 s is used in simulation of heat transfer within immersed object.

In the second parallel process, the simulation of heat transfer between the emulsion and immersed surface and the calculation of heat transfer from bubbles are carried out on one computer. The average heat transfer coefficient on the immersed surface, h_w , is calculated, depending on heat transfer coefficient of the emulsion, h_e , the heat transfer coefficient of bubbles, h_b , and bubble fraction, f_b . The result is

proposed as convection boundary condition in simulating the heat diffusion within the immersed object on another computer. Same as the first parallel process, the models are interacted via communicators and message stored in a library.

3.3 User defined functions

The simulations were implemented into Fluent CFD package. Due to the governing equations and boundary conditions in the present simulation being different from those available in the software, various user-defined functions (UDFs) shown in Table 2 and Table 3 were programmed in language C++ and integrated into a shared library that is linked with the standard Fluent executable at runtime.

Macro(User Defined Function, Parameters)	Activate in	Functions
DEFINE_INIT((Initialisation, domain)	UDF Hooks	Initialises variables; Calculate fluidising parameters
DEFINE_ADJUST(Adjust, domain)	UDF Hooks	Calculate heat-transfer coef. and heat flux
DEFINE_PROPERTY(Steel_Density, c, t)	Solid	Define solid density
DEFINE_PROPERTY(Steel_Thermal_Cond, c, t)	Solid	Define solid thermal conductivity
DEFINE_PROPERTY(Steel_Specific_Heat, c, t)	Heating Surface	Define solid specific heat
DEFINE_PROFILE(Heat_Flux, t, nv)	Heating Surface	Define heat flex

Table 2. UDFs in simulating on temperature within immersed object

Macro(User Defined Function, Parameters)	Activate in	Functions
DEFINE_INIT((Initialisation, domain)	UDF Hooks	Initialises variables
DEFINE_ADJUST(Adjust, domain)	UDF Hooks	Find the threads of boundaries Calculate radiation
DEFINE_PROPERTY(Air_Density, c, t)	Gas Phase	Define air density
DEFINE_PROPERTY(Air_Thermal_Cond, c, t)	Gas Phase	Define air thermal conductivity
DEFINE_PROPERTY(Air_Viscosity, c, t)	Gas Phase	Define air viscosity
DEFINE_PROFILE(Inlet_Vel, t, nv)	Inlet of Gas	Input fluidising velocity
DEFINE_SOURCE(Momentum_X, c, t, dS, eqn)	Porous Medium	Calculate momentum $F_{s,x}$
DEFINE_SOURCE(Momentum_Y, c, t, dS, eqn)	Porous Medium	Calculate momentum $F_{s,y}$
DEFINE_SOURCE(Momentum_Z, c, t, dS, eqn)	Porous Medium	Calculate momentum $F_{s,z}$
DEFINE_HEAT_FLUX(Heat_Flux_P, f, t, c0, t0, cid, cir)	Particle Surfaces(Wall)	Calculate radiative heat flux from particles
DEFINE_HEAT_FLUX(Heat_Flux_w, f, t, c0, t0, cid, cir)	Immersed Surface	Calculate heat flux to wall

Table 3. UDFs in simulating on the heat transfer from emulsion

4 Conclusions

The heating of an immersed object in a gas fluidised bed is a complex alternant heat transfer process that is induced by particle packets and gas bubbles. Because there is a very large geometrical size difference between the particle packet, the gas bubble and the heated object, modelling the physical phenomenon, generating mesh and grid and developing a computational method are significant to simulate the heat transfer between the immersed object and fluidised beds.

The particle packets are modelled by a porous medium close to bulk and two particle-layers near the object surface. The bubbles in contact with the object are considered as being transparent and modelled by hemispherical model. Two parallel solver processes were developed to perform the simulation of alternant heat transfer and implemented with Fluent CFD package. The methods proposed in present work were successfully used to study the heat transfer mechanism and calculate the instantaneous heat-transfer coefficient and simulate the heating process of the immersed object in fluidised beds.

References

- [1] Davidson, J. F. and Harrison, D., "Fluidization," Academic Press, London, New York, 1971.
- [2] Yang, W.-C., "Fluidization: Solids handling and processing, Industrial applications," Noyes Publications, Westwood, New Jersey, U.S.A., 1998.
- [3] Toomey, R. D. and Johnstone, H. F., "Gas fluidization of solid particles," Chem. Eng. Prog., 48, 220-226., 1952.
- [4] Kunii, D. and Levenspiel, O., "Fluidization Engineering," Butterworth-Heinemann, Krieger, Huntington, New York, 1991.
- [5] Chen, J. C., "Heat transfer in fluidized beds," Fluidization solids handling and processing, W.-C. Yang, Noyes Publications, Westwood, New Jersey, 153-208, 1999.
- [6] Saxena, S. C., "Heat transfer between immersed surfaces and gas-fluidized beds," Advances in Heat Transfer, 19, 97-190, 1989.
- [7] Howard, J. R., "Fluidized bed technology: Principles and applications," Adam Hilger, Bristol and New York, 1989.
- [8] Geldart, D., "Types of gas fluidized," Powder Technology, 7, 285-292, 1973.
- [9] Gao, W. M., et al., "Numerical simulation and mechanism of heat transfer in quenching fluidised beds," Proceedings of the 4th international conference on quenching and the control of distortion, Beijing, 137-142, 2003.
- [10] Gao, W. M., et al., "Numerical Study of the Conduction and Convection between Immersed Object and Gas Fluidised Bed," 7th Biennial Conference on Engineering Systems Design and Analysis, Manchester, United Kingdom, ESDA2004-58264, 2004.
- [11] Yoshida, K., et al., "Mechanism of bed-wall heat transfer in a fluidized bed at high temperature," Chemical Engineering Science, 29, 77-82, 1974.
- [12] Fluent-Incorporated, "Gambit 1.2," 2000.
- [13] Fluent-Incorporation, "Fluent 5.504," 2001.
- [14] Gao, W. M., et al., "Numerical simulation of heat and mass transfer in fluidised bed heat treatment furnaces," Journal of Materials Processing Technology, 125-126, 170-178, 2002.